SSRG International Journal of Civil Engineering
ISSN: 2348-8352/ https://doi.org/10.14445/23488352/IJCE-V13I2P109

Volume 13 Issue 2, 117-131, February 2026

Original Article

Explicit Dynamic Analysis of a Steel Column Subjected to Near-Field Explosion

Deepak G. B[1], Sangita S Meshram[2], Gopal Malba Alapure[3], S. Sudhakar[4], Saurabh S Joshi[5], Prashant Sunagar[6], Sughosh P[7]

[1]*Department of Civil Engineering, Dayananda Sagar Academy of Technology and Management, Bangalore*
[2]*Department of Civil Engineering, Yashwantrao Chavan College of Engineering, Nagpur, Maharashtra*
[3]*Department of Civil Engineering, Dhole Patil College of Engineering, Pune, Maharashtra*
[4]*Department of Civil Engineering, School of Engineering & Technology, Sandip University, Nashik*
[5]*Department of Civil and Environmental Engineering, KIT's College of Engineering (Empowered Autonomous), Kolhapur, Maharashtra*
[6]*Department of Civil Engineering, Sandip Institute of Technology & Research Centre, Nashik, Maharashtra*
[7]*Department of Civil Engineering, Manipal Institute of Technology, Karnataka*

[6]*Corresponding Author : prashant.sunagar@sitrc.org*

Received: 18 November 2025 Revised: 20 December 2025 Accepted: 21 January 2026 Published: 11 February 2026

Abstract *- Bomb attacks inside or near buildings can cause Catastrophic damage to structures inside and outside the structure, collapse walls, blow up large sections of windows, and disrupt security systems. The casualties of the victims can be multiplied, including the direct effects of the explosion, the destruction of structures, and the impact of debris. Indirect effects can be combined to prevent a rapid evacuation, resulting in more casualties. In addition, the high loads due to chemical gas explosions can cause dynamic loads in many structures that are greater than the original design loads. In view of the threat of these extreme loading conditions, the behavior of the building structure under explosive charges is studied. A column under axial force and the blast load were simulated and analyzed. The ANSYS finite element platform is used to model columns with various support end conditions.*

Keywords *- ANSYS, Blast Loading, FEM, Extreme Loading, Buildings.*

1. Introduction

With increased urban density, industrial accidents, and asymmetric safety threats, both intentional and accidental explosive loading against civil infrastructure is increasingly prevalent. Columns, as vertical elements, are most vulnerable to near-field blast loading relative to high strain rates, impulsive pressure loading, and the nature of physical loading through axial force. However, established structural design code language and corresponding assumptions for intervention relative to gravity loading, loading phenomena induced by material degradation, and seismic loading fail to address the transient, nonlinear loading response for explosive events since existing language focuses on what can be quantified under quasi-static conditions.

Recent advancements in blast-resistant design primarily concern global stability assessment, façade response, or shear wall applications; however, secondary investigations fail to emphasize detached columns subjected to simultaneous axial force and near-field blast loading. Furthermore, recent developments that emphasize single application considerations support boundary conditions and cross-sectional shape implement idealized end restraints, either fixed or pinned, without relative determination of realistic end restraint effectiveness on wave propagation through non-finite deformation, deformation concentration, and failure modes.

In addition, prior to 2018, many of the numerical studies indicate simplistic pressure-time functions or quasi-static applications that either fail to ramp up pressure relative to frequency and throughout the trajectory of loading or fail to accrue response increases relative to material degradation throughout the loading time. Since 2018, phenomenal developments in explicit solvers have addressed near-field blast loading events with accuracy; however, finite element studies of steel columns with various geometrical considerations under the same loading events remain few and far between.

Therefore, the contribution of this study is to bridge the existing gaps in literature through an explicit, dynamic, detailed finite element analysis on near-field blast loading on axially loaded steel columns using a validated approach within the realm of ANSYS Explicit Dynamics software to determine the result in deformation, stress, and strain response based on proximity to source and Angle of incidence generated, as well as cross-sectional profile and support considerations. Ultimately, the results presented herein generate new opportunities for quantifying resiliency at the column level relative to design efforts on those

infrastructures of most significant interest, with comparisons made possible relative to contemporaneous literature on resiliency, which indicates components of localized interest must survive extreme loading before progressive collapse is inevitable.

1.1. Novelty of the Present Study

Where previous studies explore world framing actions or individual boundaries, this study establishes a relative investigation of blast response amongst several steel column cross sections with an equivalent near-field explosive load. This research contributes:

- Relative comparison of open (I, H) and closed (circular, square) sections of equivalent cross-sectional area under the same blast loading
- Relative comparison of blast loading angle of incidence (0°, 45°, 90°) on the extent of increase in deformations and stress redistribution
- Relative comparison of boundary conditions (unevenly supported columns with guided motion to one side) on dynamic response, when many papers assume boundary conditions do not matter
- A high-fidelity explicit dynamic modeling for stress wave propagation, plastic hinge formation, and strain failure

This is significant to the field for a critical level of insight into column performance under blasts that informs performance-based protective design.

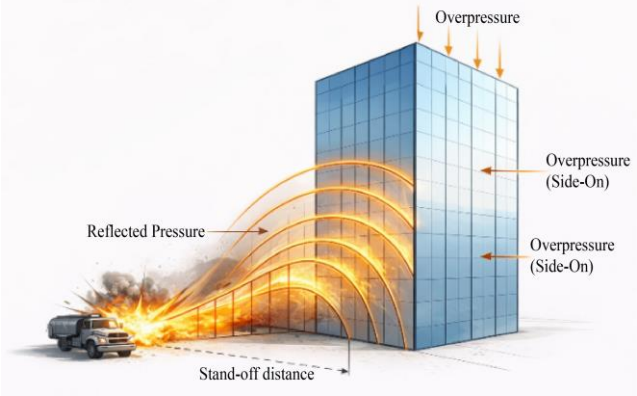

Fig. 1 Blast load effects on a building

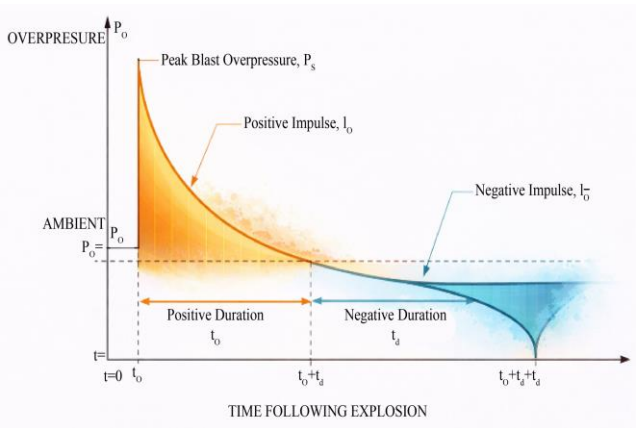

Fig. 2 Pressure-time history of pressure from an explosion

2. Literature Review

With the increasing susceptibility of urban fabric to extreme impulsive threats, the behavior of steel structural members under near-field explosion loading is an expanding field of study. As a primary vertical load-bearing member and anticipatory component to progressive collapse, steel columns serve as an experiential, numerical, and analytical focal point for research that designs against or seeks to characterize blast response mechanisms, damage development, and vulnerability or amplified tolerance.

2.1. Experimental Investigations of Blast–Structure Interaction

Many experimental studies provide a foundation for real-explosive blast-structure interaction and subsequent analytical and numerical validations. One in-field laboratory study performed detonative explosives on steel members, measuring time histories of displacements, velocities, and accelerations. It was found that a single-degree-of-freedom idealization can simplistically predict observed displacements within elastic response conditions reasonably well; however, with increasing accuracy of a plastic response via localized damage, this was not the case [14].

Research on full-scale steel I-section columns under blast loading found that with loading wave durations within the 10-40 ms threshold compared to lower durations for pressure pulses, the performance of these structures was more sensitive to axial distance and incident angle of loading than other variables; in fact, [Q]—the urging force—was larger in oblique compared to orthogonal blast housing, implying the need for critical design of column-level integrated blast resistant systems for idealized assumptions of no failure under perfect, favorable pressure exposure; this lower extreme pressure demand would seem more realistic.

Increasing quantities of diagnostics measured full-field assessments of DIC—digital image correlation—where high-speed stereoscopic captured localized deformation and particle velocity fields on plates under dynamic loading to better understand rapid kinematic evolution causing strain localization and rapid fragmentation, which improves constitutive modeling [21].

2.2. Wave Physics and Pressure–Time Measurement

Assessing blast waves is critical to understanding pressure assessment; utilizing tracer particles and real-time measurements of particle trajectories allows researchers to visually assess unsteady shock waves where flow-field properties of pressure density, temperature, and particle velocity all evolve. It's been determined through pioneering work that the pressure time histories established experimentally possess comparable accuracy to instrument derivations and well-rounded physical representations of the blast [2].

Applied engineering factors depend on pressure over time functions achieved through empirical readings; one study tried to experimentally derive equivalent pressure

duration and width as hypothesized [4] before composite performance analysis of data using national design criteria substituted with derived charge weight (and subsequent realistic scaled distance) yielded equivalent nonlinear histories from critical performance assessment realized for base shear, story displacement and uniform load from resultant force.

2.3. Numerical Explicit Dynamic Modeling

Modeling gives researchers the ability to supplement these assessments, and finite element methods using explicit dynamics have become a standard tool for blast structure interaction approximations; solvers consider proper appearance, shock wave, and strain rate behavior, contact interaction, and progressive failure [3, 4].

Relative studies were done on perforated steel columns under near-field explosions where damage occurs in defined stages and shock gap initial loading is seen first then through axial loading over time; boundary conditions were significant as the pin connection fixed end derived less residual capacity than the pin connection alternative; retrofitting web holes would negate damage tolerance decrease while additional rigid shear connections would substantiate relative additional blast tolerance when extreme [22]. Steel columns connected to composite systems have been gaining traction relative to concrete-filled dual skins, where damage occurs from composite concrete shear (crushing, cracking) and steel yielding; models hypothesized strain rate sensitivity, which accounted for impulse loading, compared well to experimental findings, which inform specific material modeling for performance [1].

2.4. Analytical and Probabilistic Assessment

In addition to established damage prediction probabilities, there is an analytical and probabilistic approach that accounts for resistors' responses to uncertain blast magnitude or material characteristics. Monte Carlo simulations with finite element explicit modeling derived damage exceedance probabilities based on random distributions, which ultimately derived safe scaled distances for different types of steel columns in a derived instantaneous criteria application to practical implementation with low error [21].

Simplified analytical models are developed through parametric time history analysis; a comprehensive study into the ultimate response of Cantilevered Wall Systems, where the velocity response spectrum corner period is the governing determiner based upon blast response characteristics from a load perspective, provides a more realistic capacity-spectrum-based design [6] than pure pictorial image history of finite simulations [9].

2.5. Structure Configuration and Multi-Hazard Investigation

In lateral load resisting systems, for example, plate shear walls have a hybrid benefit. However, combined extremes reduce their efficacy as the excessive demand on columns from a stiffness standpoint deteriorates generic efficiencies from a construction perspective. Column thickness may be too large, or stiffness forces may be too high; therefore, the configuration of these structures must be better determined with an ideal thickness choice [3].

Studies into other hazards show that post-blast fiber-based effects relative to fire decrease level resistance when post-blast damage is substantial, when other proportional levels are taken into account [7, 9]. For example, studies of underwater (relative to near-field explosions) steel concrete slabs show that the additional danger of bubble pulsation damage in addition to standard shock pressure confounds the response from the initial explosion [16].

2.6. Summary and Research Gap

There is ultimately much research to support the understanding of steel columns under near-field explosion by means of blast magnitude, configuration, and delimited characteristics of deflection resulting regardless of boundaries sustained that inspire deformation as a function of strain rate sensitivity during the application of forces and post-blast loading event. There are few comparative impact studies between cross-sectional configurations equally subjected to near-field blasts with proper support boundary conditions that possess configuration extremes that convey cut downs. In addition, despite research trying to approximate empirical results and finite element explicit dynamic analysis, trial and error-driven conclusions emphasize practical application where time-across-deflection increases damage tolerability probability, where idealized excess deformation vulnerability invokes a deformation-across-time based requirement; neither approach localized stress redistribution into account. This proposed research will fill the gap with critical implications for performance-based design fundamentals, suggesting that the dynamics of steel columns in near field blasting are contingent upon complex interactive patterns, but not assuming between excavation boundary conditions and geometry type. Despite much empirical research into blast-resistant structures, the synergistic influence of support conditions with cross-sectional geometry and near-field blast response for all axially loaded steel columns is still under-represented.

3. Methodology

3.1. Analysis of a Steel Structure in ETABS for Normal Design Loads

A steel structure of G+3 stories is analyzed in ETABS. It is analyzed for normal design loads, such as dead load and live load, considering it as a residential building. The material properties of concrete used in a slab of thickness 200mm are taken as M30 grade, and the steel used for the column and beam is Fe345 grade.

Steel sections for beams and columns are defined by ISHB, ISLB, ISMB, and ISWB sections. A steel frame structure with 4 bays and 4 stories with a storey height of 3m and a width of 4m is modeled with a slab thickness of 200 mm.

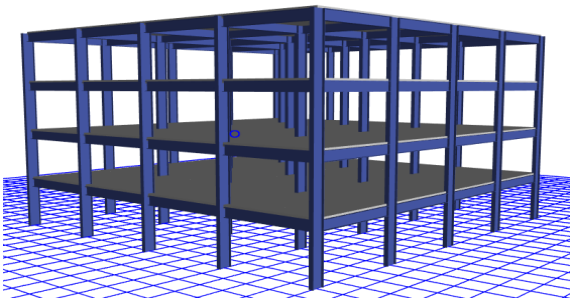

Fig. 3 Rendered view of steel frame structure

Live loads are considered according to IS 875 (Part 2) - 1997 for a residential building. LL of 3 KN/m^2 with FL of 1.5 KN/m^2 is applied on the slab and wall load of 12 KN/m put on the beams, except for the parapet wall of 5 KN/m at the top.

Analysis has been made for load combinations DL, Dl+LL, 1.5DL, and 1.5DL+1.5LL. Beams and column sections are changed, and frame members are passed with ISMB450 and ISMB500 sections in the design. Columns 7, 8, 9, 12, 13, 14, 17, 19, and 20 are to be more critical when compared to others in terms of axial column forces and section requirements. As shown in Figure 4, columns 8 and 19 are more critical. One of these columns is considered a critical column, with an axial column force of approximately 1472 kN. Column number 19 is considered the critical column for the analysis against the blast loading.

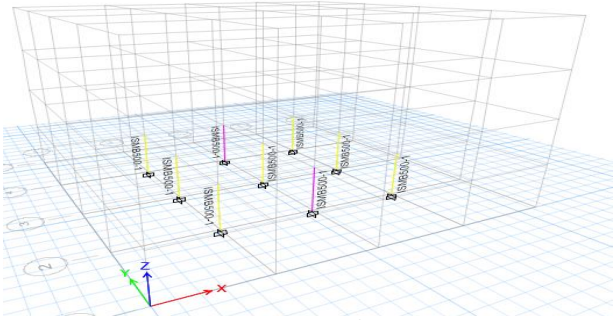

Fig. 4 Critical columns after the design

After selecting a critical column section, ISMB500 from ETABS, we need to model a 3m-high column for different section shapes, such as I-section, H-section, circular-section, and square-section columns. All these columns have the same cross-sectional area of 110.7cm^2.

3.2. JWL Equation of State

The Jones–Wilkins–Lee equation is used to define the ignition of explosives.

$$p = A\left(1 - \frac{w}{VR_1}\right)e^{-VR_1} + B\left(1 - \frac{w}{VR_2}\right)e^{-VR_2} + \frac{we_0}{v} \quad (1)$$

The ratio $V = \frac{\rho_e}{\rho}$ is defined by using ρ_e= density of the explosive rock-hard part and ρ = density of the detonation products.

3.2.1. P-α Equation of State

The RHT model utilizes the p-α equation of state introduced by Herrmann. The porosity α is defined as the ratio of the specific volume of the porous material (v = 1/ρ) to that of the matrix material (Vsolid = 1/ρsolid). In the CONC-35 parameter, the values of ρ_{solid} = 2.75 g/cm^3 and ρ_{porous} = 2.341 g/cm^3.

$$\alpha = \left(\frac{v}{V_{solid}}\right) = \left(\frac{\rho_{solid}}{\rho}\right) \quad (2)$$

3.2.2. Polynomial Equation of State

The RHT model employs the polynomial equation of state for the matrix material, given in the equation.

$$p = \begin{cases} A_1 \cdot \mu + A_2 \cdot \mu^2 + A_3 \cdot \mu^3 + (B_o + B_1 \cdot \mu) \cdot \rho_o \cdot e & if\ \mu \geq 0 \\ T_1 \cdot \mu + T_2 \cdot \mu^2 + B_o \cdot \rho_o \cdot e & if\ \mu < 0 \end{cases} \quad (3)$$

Where, $\mu = \frac{\rho}{\rho_o} - 1$ is defined by current density ρ and density ρo at zero pressure.

3.3. Material Model

While solids tend to behave elastically, they will apply stress conditions that exceed yield stress and behave plastically under highly dynamic loading. The mesh material is nonlinear elastic-plastic. The subsequent Table 1 presents the material properties of TNT, Structural Steel, and Concrete.

Table 1. Material properties of explosive TNT

Material	Explosive TNT (trinitrotoluene)
Density	1630 kg/m^3
A	37 × 10^{10} Pa
B	3× 10^{10} Pa
R_1	4.15
R_2	0.9
W	0.35
v	6930 m/sec
E	3681000 J/kg
p	2× 10^{10} Pa

3.4. Stress-Strain Curves

Stress-strain curves of concrete of several grades found from typical uniaxial compression tests are shown in Figure 5. The maximum stress is reached at a strain of 0.002.

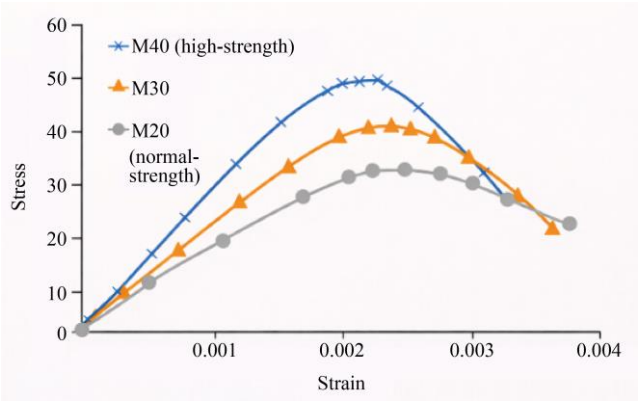

Fig. 5 Stress-strain curves of concrete

Steel exhibits plastic behavior when subjected to high-pressure levels; it does not return to its initial shape but instead undergoes permanent plastic distortion. Uniaxial stress-strain curves are shown in Figure 6 for various grades of steel.

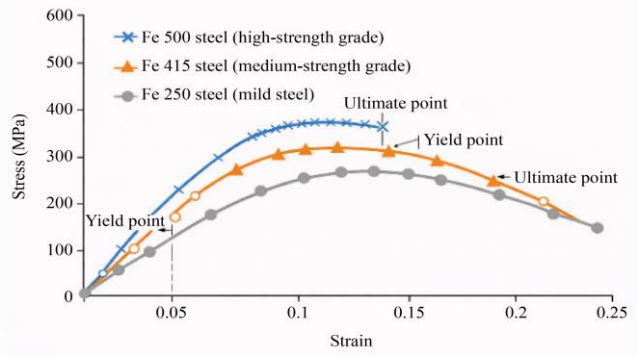

Fig. 6 Uniaxial stress-strain curves of steel

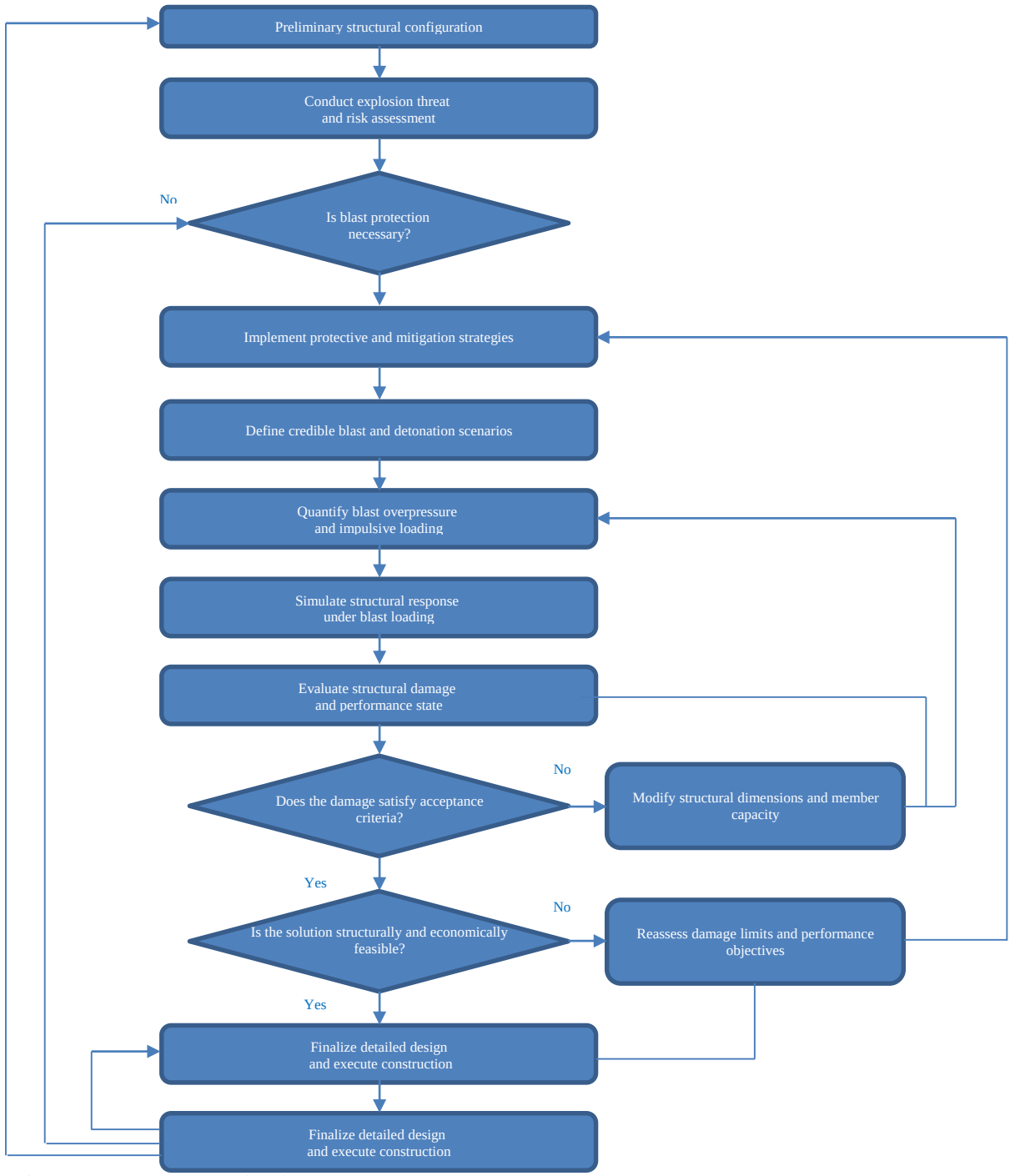

Fig. 7 Performance-based design workflow for blast-resistant structures incorporating threat assessment, nonlinear response evaluation, damage acceptance & iterative structural optimization

4. Blast Simulation

4.1. Geometry Modelling

The 3D solid geometry of the steel column and solid TNT are modeled using the geometry module in ANSYS Explicit Dynamics. The TNT model is square in section, with a dimension of 395 mm, calculated based on the density and the amount of charge weight to be loaded on the column members.

4.1.1. Angle of Blast Incidents

The blast TNT is applied from three different angles to a single column. The angles of incidence are taken at 0°,45°, and 90°. For that, columns are rotated at a particular angle while modeling in geometry. Philosophy in the design of the building is finest offered in the form of a flowchart. The flow chart shows the activities and their order for shielding people, assets, and the business.

4.2. Modeling Using Ansys

ANSYS is an FEM software that provides a numerical solution to various structural problems. The library consists of various elements. For the numerical modeling of each of them, three-dimensional solid elements SOLID65 were used to model the nonlinear response of concrete, and three-dimensional beam elements LINK8 were used for the modeling of reinforcements.

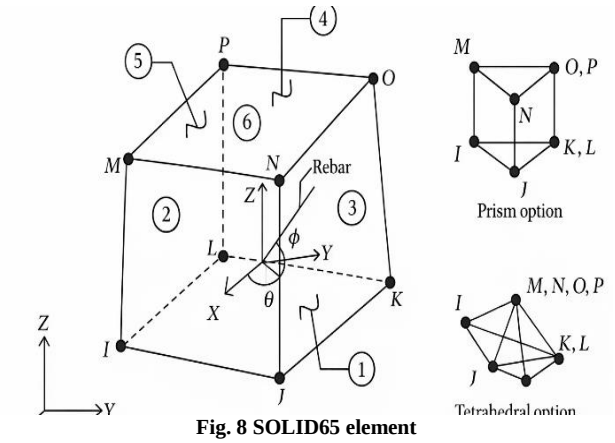

Fig. 8 SOLID65 element

4.2.1. Link8

Link8 is a 3D beam element. It is used to simulate reinforcement in concrete. Each node has three degrees of freedom.

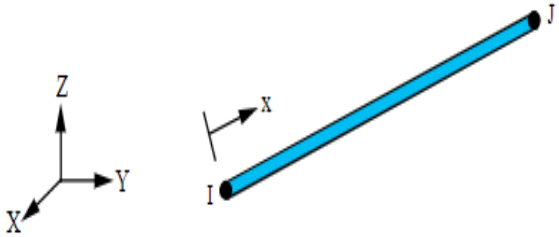

Fig. 9 Link8 Element

4.2.2. Multi-Crack Model

The multi-linear stress-strain execution needs the starting point of the curve to be well-defined by the user.

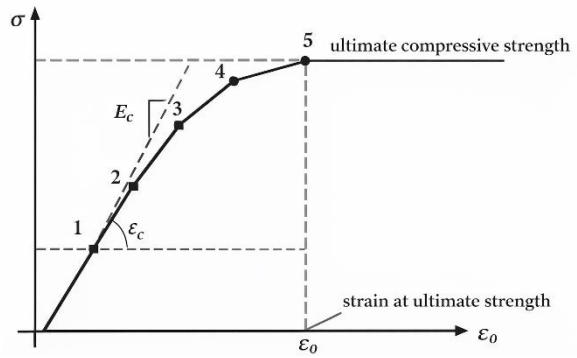

Fig. 10 Multi-linear Isotropic Stress-Strain Curve

4.2.3. Blast Loading on Columns

Four types of different shape column dimensions are considered to load blasts at different angles of incidence and different support conditions. A charge weight of 100kg of TNT and a standoff distance of 2m is considered for every condition to know the response of the column to the blast load. The JWL equation of state is used to define the TNT material properties. The detonation point is set inside the TNT material to simulate the explosion.

4.3. Geometric Models of Different Types of Columns

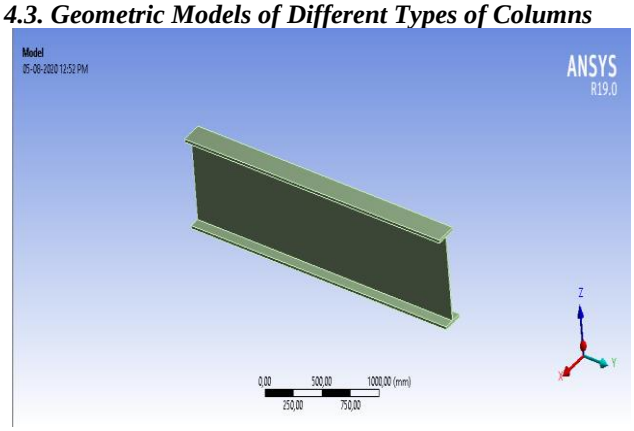

Fig. 11 Geometric model of I-section steel column in ANSYS

Explicit dynamic analysis was conducted through ANSYS Explicit Dynamics, accounting for the nonlinearities introduced through high strain rates and transient stress wave propagation. For the analyses, structural steel was defined as a nonlinear elastic–plastic material with isotropic hardening, and the strain rate effects were accounted for inherently through the explicit time integration.

Appropriate boundary conditions were applied to reflect realistic column end restraints that would be typical in a framed structure. Prior to detonation, a normalized axial load was applied to ensure proper stress state interaction was maintained during the pre-stress phase of the analysis. The TNT detonation was modeled using the JWL equation of state, which effectively estimates pressure–time history and shock wave propagation.

Mesh sensitivity analyses were performed to ensure numerical stabilization and convergence of maximum response values.

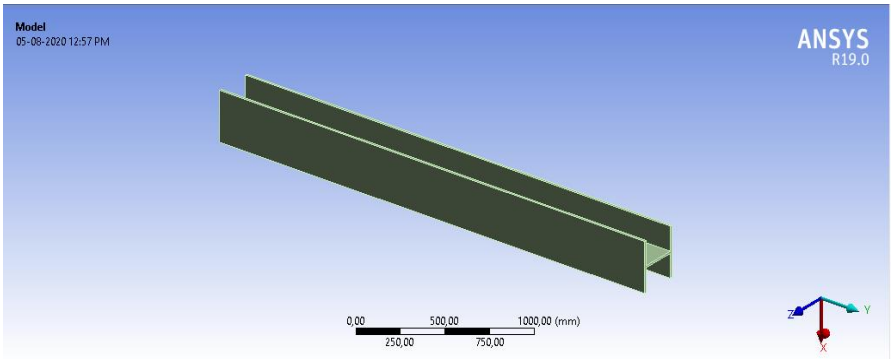

Fig. 12 Geometric model of H-section steel column in ANSYS

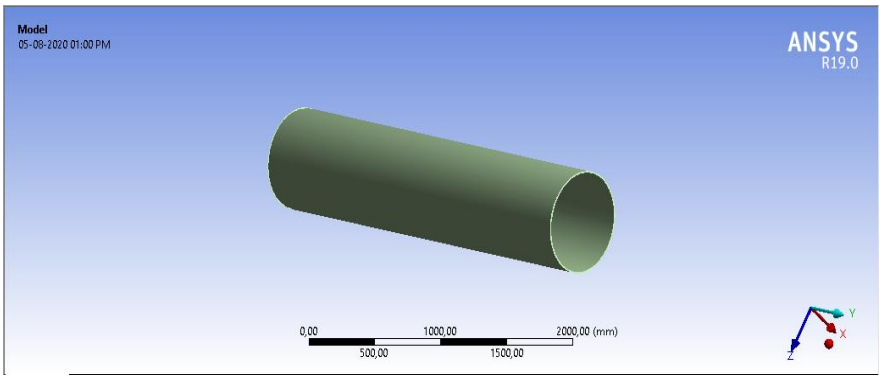

Fig. 13 Geometric model of circular section steel column in ANSYS

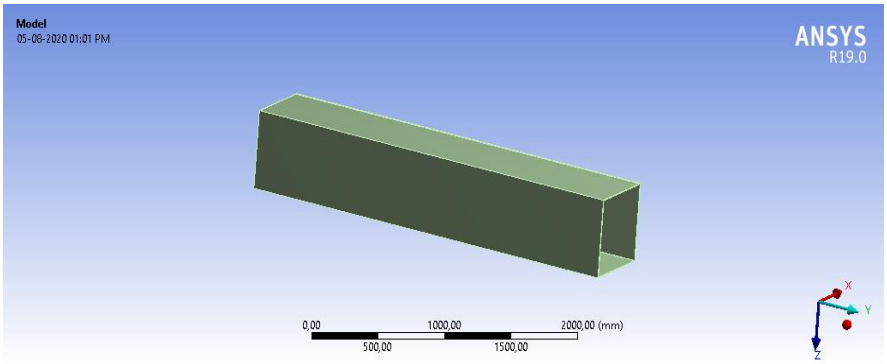

Fig. 14 Geometric model of square section steel column in ANSYS

4.4. Deformation Patterns

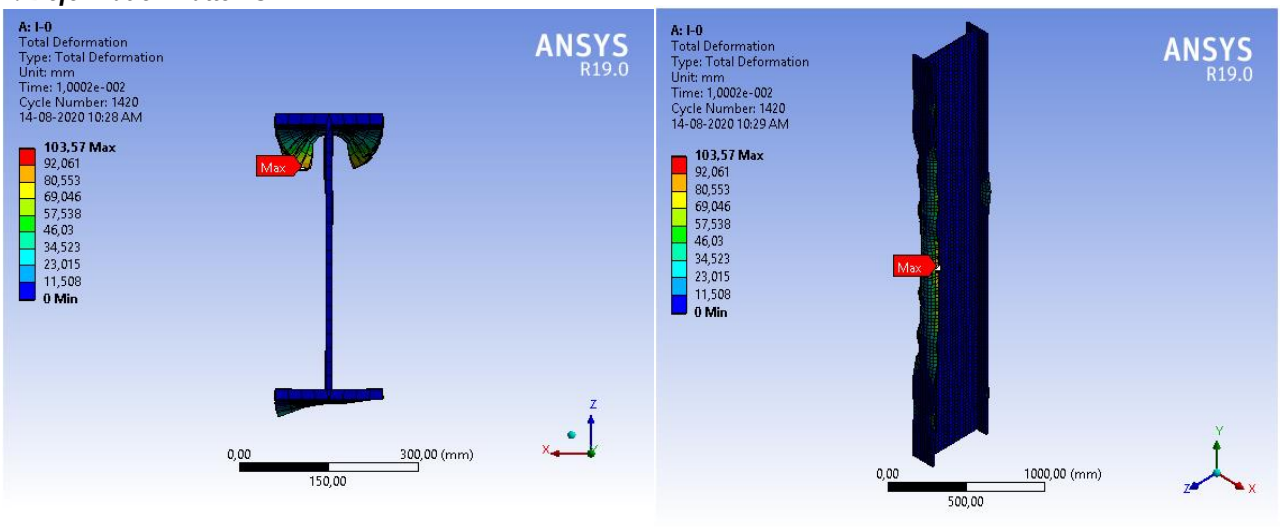

Fig. 15 Deformation pattern for a section column at 0° angle of incidence

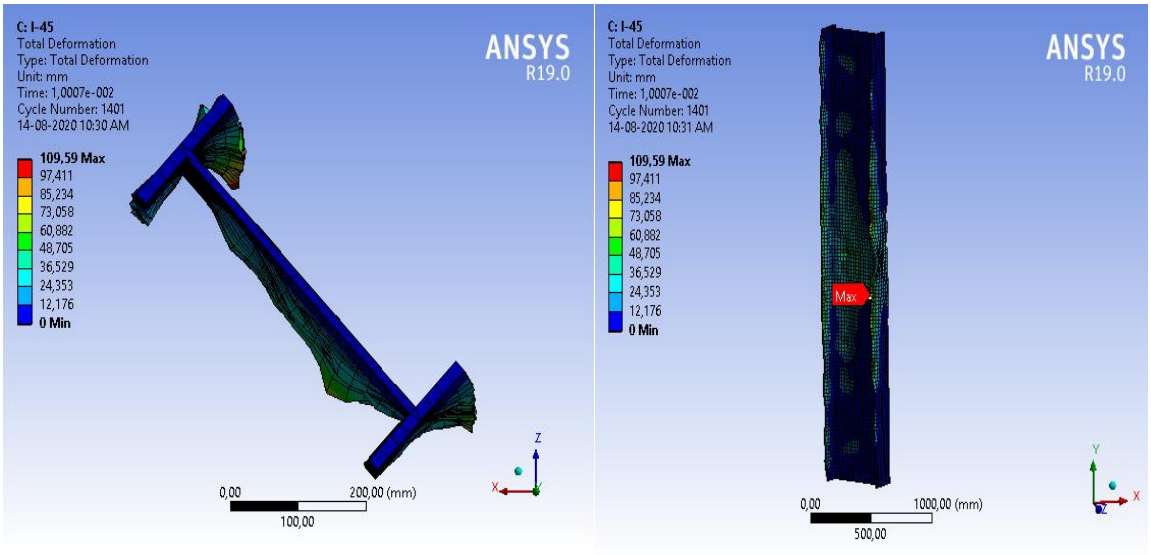

Fig. 16 Deformation pattern for I-section column at 45° angle of incidence

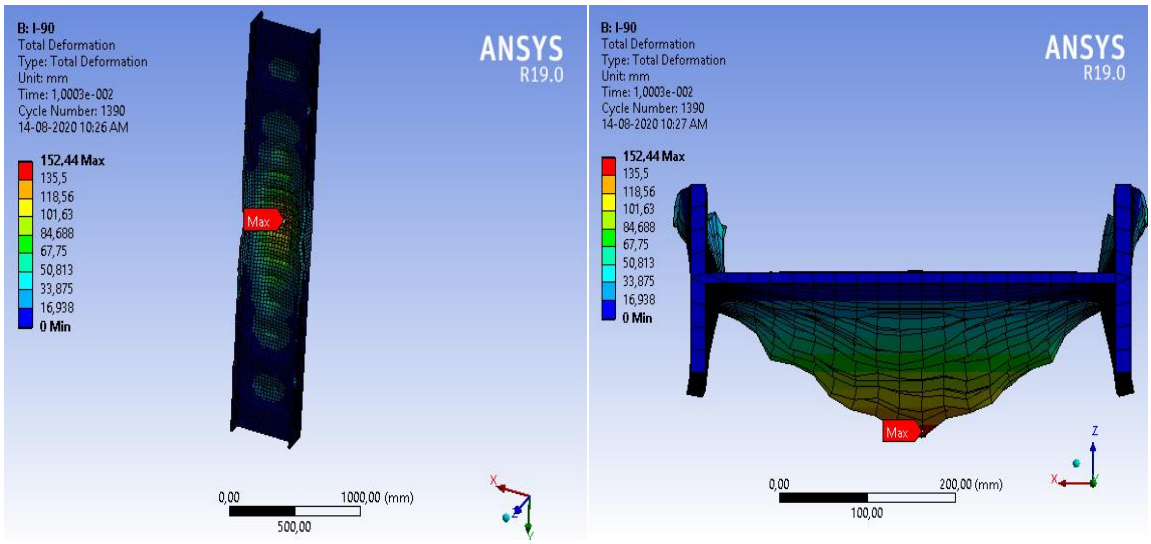

Fig. 17 Deformation pattern for a section column at a 90° angle of incidence

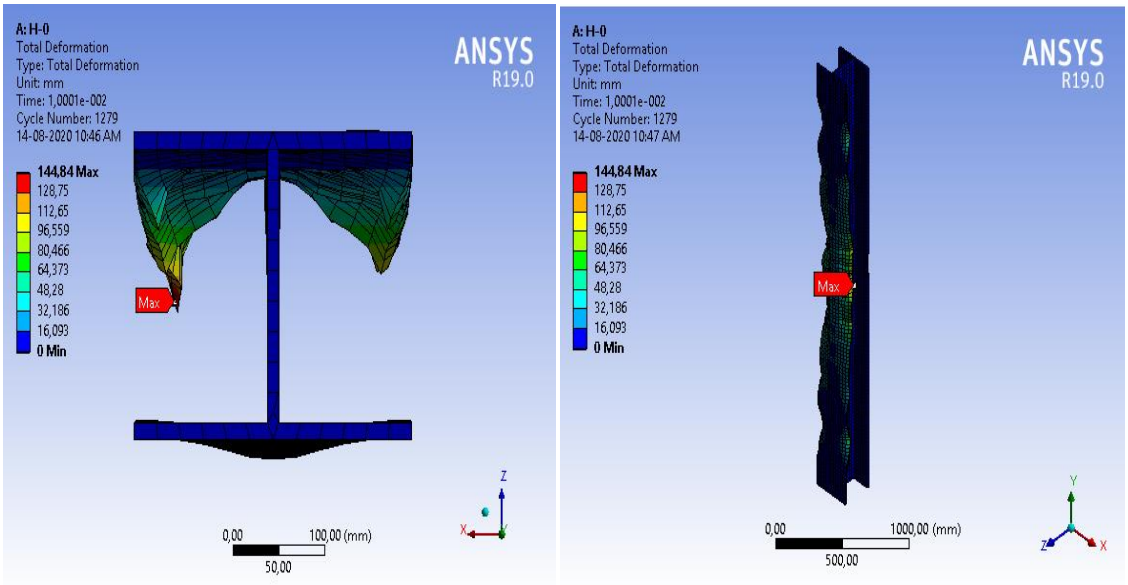

Fig. 18 Deformation pattern for H-section column in 0° angle of incidence

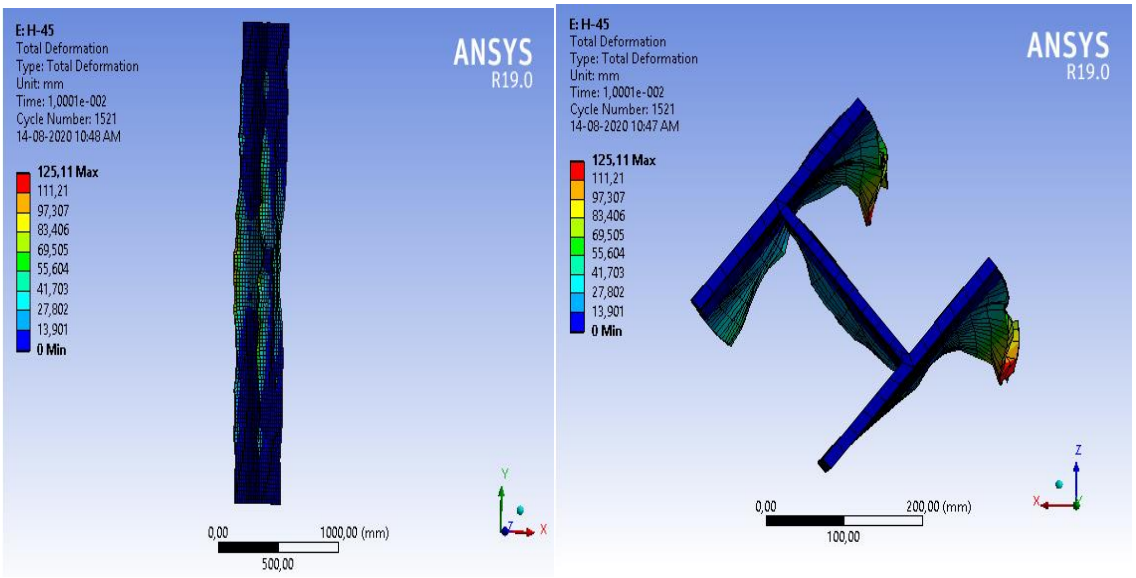

Fig. 19 Deformation pattern for a section column at a 45° angle of incidence

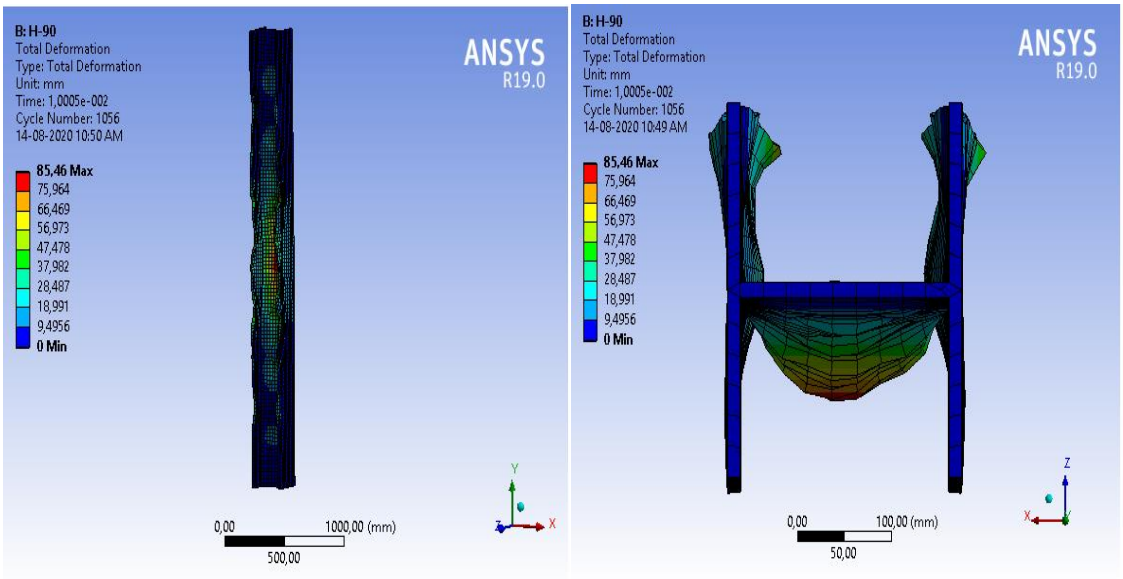

Fig. 20 Deformation pattern for H-section column at a 90° angle of incidence

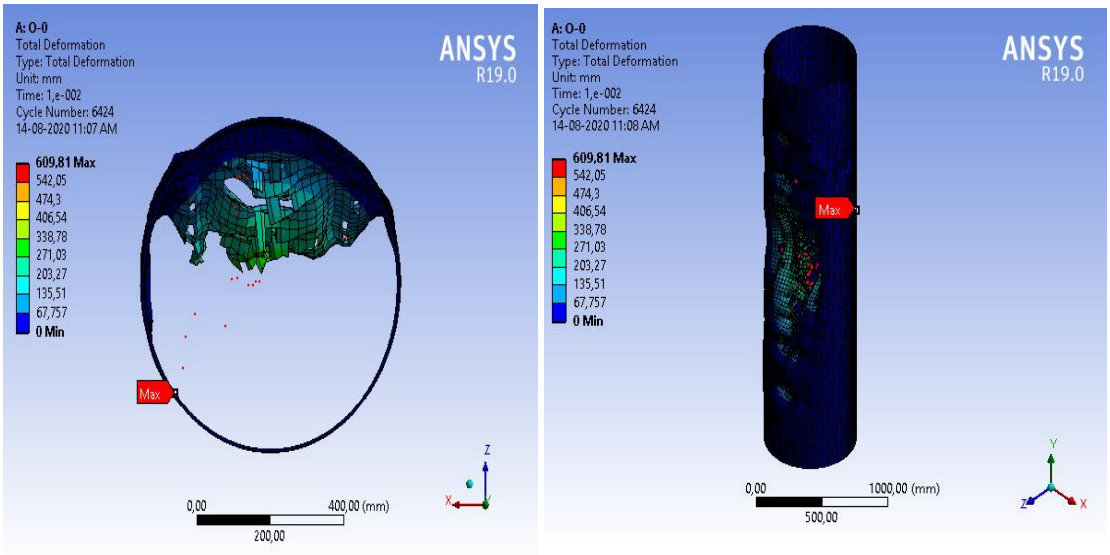

Fig. 21 Deformation pattern for circular-section column

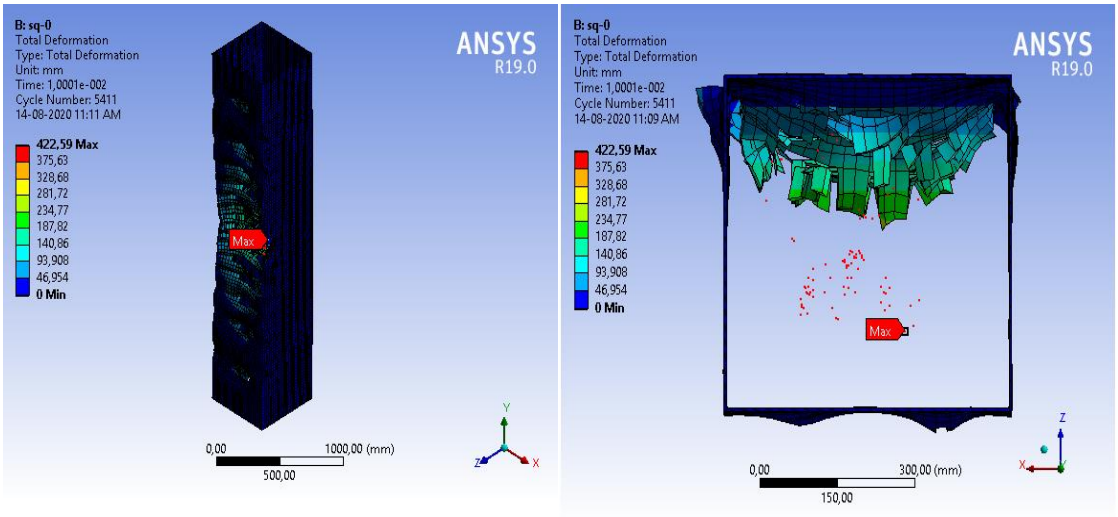

Fig. 22 Deformation pattern for square-section column in 0° and 90° angle of incidence

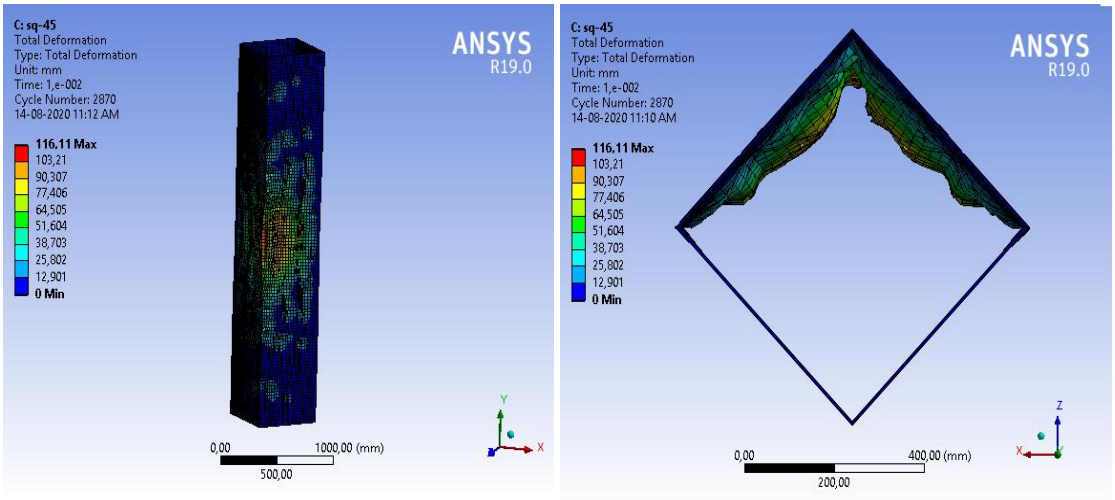

Fig. 23 Deformation pattern for square-section column in 45°angle of incidence

5. Results

5.1. Deformation (mm)

Table 2. Deformation for 0° 45° and 90° angle of incidence

Angle of incidence (degrees)	0°	45°	90°
I section	103.57	109.59	152.41
H section	144.84	125.11	85.46
Circular section	609.81	609.81	609.81
Square section	422.59	116.11	422.59

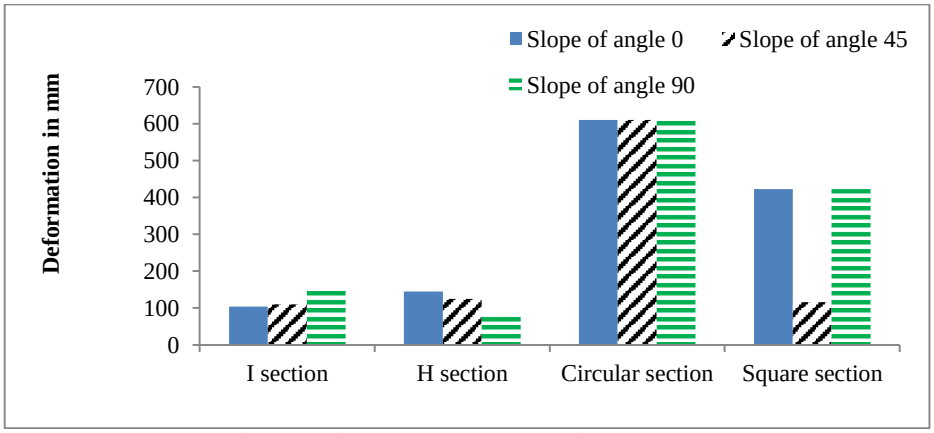

Fig. 24 Deformation for 0°, 45° and 90° angle of incidence steel sections

From the above figures, we can observe that deformation is greater in closed sections, such as circular and square sections, than in open sections, like I-section and H-section. When we compare I and H sections, we can see that the deformation of section I is less in case 0° Angle of Incidence and more in 90° Angle of Incidence. In section H, deformation is more at 0° Angle of Incidence and less at 90° Angle of Incidence, and is almost equal at 45° Angle of Incidence. From these, we can say that the deformation is greater when the area of exposure to blast is greater, and the pressure exerted on that area is also greater. In a circular section, the deformation has changed for every Angle of Incidence, and the area of exposure is also larger, so the deformation is also greater. In a square section, the deformation is greater when the exposed area is directly opposite to the blast pressure. At a 45° Angle of Incidence, the deformation is less since the areas are slightly inclined for the line blast pressure, which we can also observe in the case of I and H sections for a 45° Angle OF Incidence.

5.2. Equivalent (Von-Mises) Stress (MPa)

Table 3. Equivalent Stress for 0° 45° and 90° Angle of Incidence

Angle of incidence	0°	45°	90°
I section	1098.1	1148.8	1190.6
H section	1145.8	1583.4	1089
Circular section	1166.9	1158.2	1158.2
Square section	1197.9	1102.5	1188.7

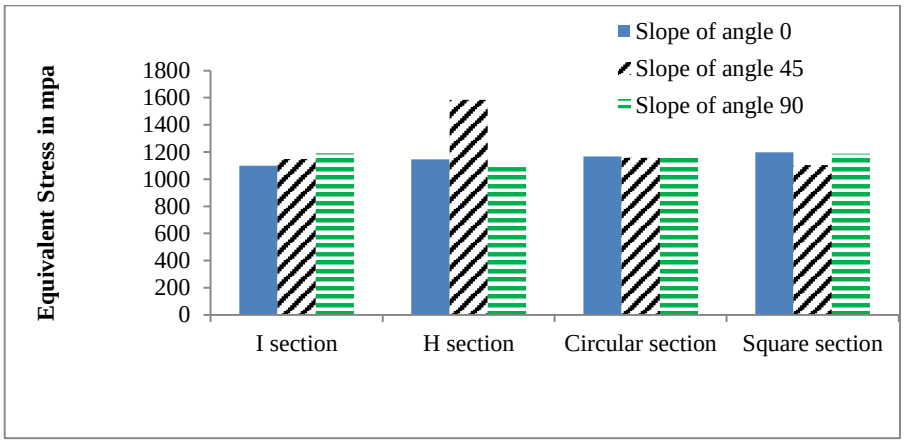

Fig. 25 Equivalent stress for 0° 45° and 90° angle of incidence steel sections

We know that equivalent stress represents the yielding point of a ductile material for multi-axial loading. Due to blast pressure, the steel sections are starting to yield at several stress points. From the above charts, we can observe that the steel section material yielded at maximum stress. The I-section and circular sections did not yield to maximum stress before entering the plastic region. Stresses are higher in the square section for 0° and 90° angles of incidence. The H-section column has yielded to the maximum stress value in the case of a 45° angle of incidence. Equivalent stresses in the circular section column are less than those in the other section in every case.

5.3. Equivalent (Von-Mises) Strain

Table 4. Equivalent strain for 0° 45° and 90° angle of incidence

Angle of incidence	0°	45°	90°
I section	0.43521	1.508	0.5042
H section	1.9178	1.9357	0.49402
Circular section	1.2335	1.2335	1.2335
Square section	1.6064	1.6004	1.6064

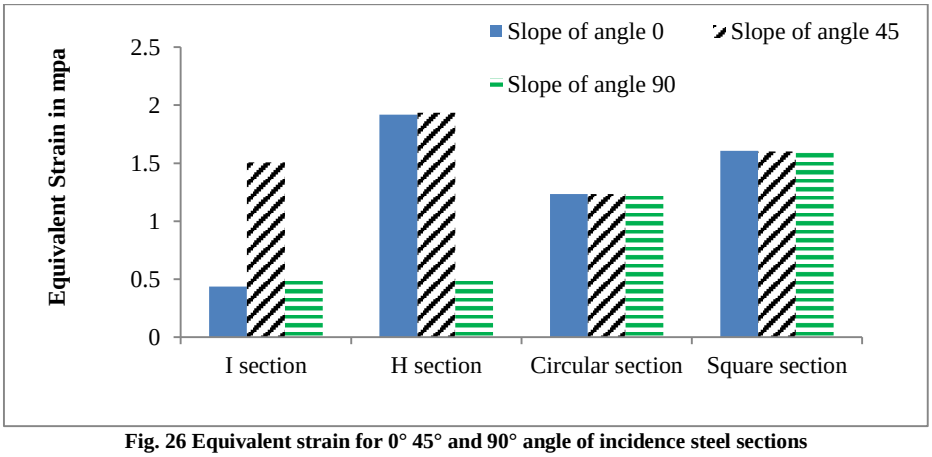

Fig. 26 Equivalent strain for 0° 45° and 90° angle of incidence steel sections

Equivalent strain values are varied for different cross sections, of course, but the variation is also noticed in the case of different Angles of Incidence. As it is in the deformation parameter, strain values are less in section I columns and more in section H columns and square section columns. For every case of the Angle of Incidence in a circular column, strain values are attained. It may be due to the dimensions of deformed parts like flange, web, tube thickness, etc. In the H section column, the strain value is much higher at a 45° Angle Of Incidence.

5.4. Maximum Principal Stress (MPa)

Table 5. Maximum principal stress for 0° 45° and 90° angle of incidence

Angle of incidence	0°	45°	90°
I section	2672.3	1241,47	1294.7
H section	1259.6	1203.2	1168.1
Circular section	1335.6	1335.6	1335.6
Square section	1291.5	1455.4	1291.5

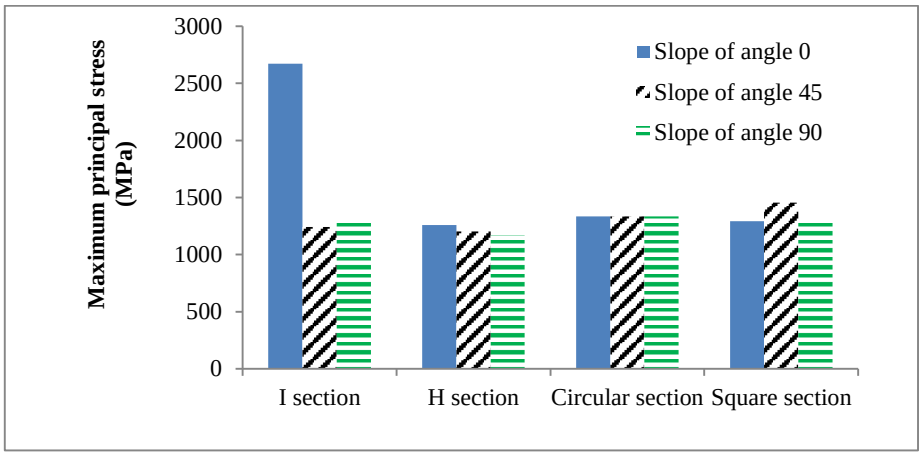

Fig. 27 Maximum principal stress for 0° 45° and 90° angle of incidence steel sections

Principal stress is everyday stress, where shear stress is zero. Max principal stresses obtained from the analysis are more than the value of equivalent stresses. From the above plots, we can see the variation of the maximum principal stresses with respect to support conditions and the Angle of Incidence.

Max principal stresses are higher in I-section columns in the case of 0° and 90° Angles of Incidence. For square-section columns, the maximum principal stresses are higher in the case of a 45-degree Angle Of Incidence. With the change in support conditions, stresses are decreased for every change. The stresses are less in the case of a 45° Angle Of Incidence, i.e., when the blast is applied from a 45° angle.

5.5. Maximum Principal Strain

Table 6. Maximum principal strain for 0° 45° and 90° angle of incidence

Angle of Incidence	0°	45°	90°
I section	0.22258	1.1887	0.66902
H section	1.4152	1.3854	0.3686
Circular section	0.64073	0.64073	0.64073
Square section	1.1715	1.018	1.1715

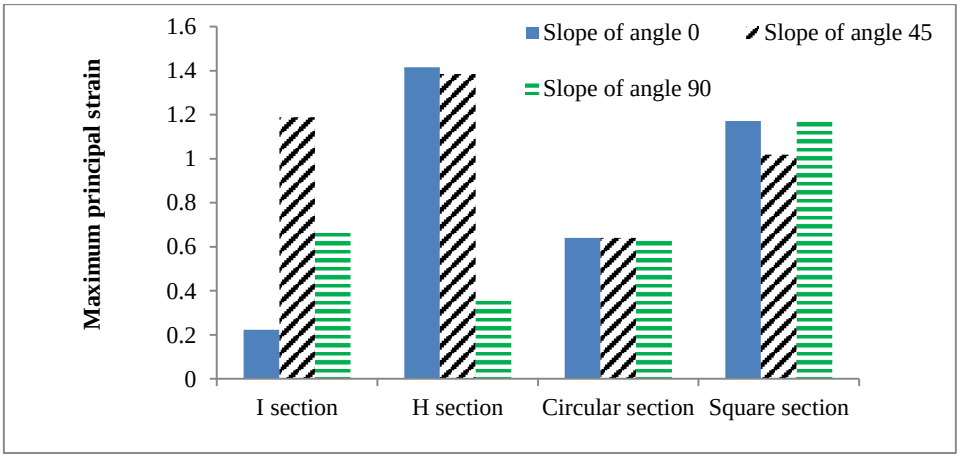

Fig. 28 Maximum principal strain for 0° 45° and 90° angle of incidence steel sections

Variation of the maximum principal strains is plotted in the above charts. Strains are varied with section changes, Angle of blast incidence, and support conditions. Strains are more in the case of 0° and 45° angles of blast incidence, especially for an H-section column. In square-section columns, the strains obtained are greater in all three cases of

blast incidence angle. Circular-section columns exhibited the same amount of strain values. By comparing the I and H section column results, we can conclude that the column with the maximum flange width exhibited the greatest strain. It is different in the case of web parts. We can also observe that the strain value in the case of an I-section column with a 45° angle of blast incidence exhibited more strain values.

5.6. Normalized Response Metrics and Statistical Validation

Performance measures of normalized deformation and stress responses were used for relative comparison of different steel column designs and end boundary conditions. These dimensionless performance measures reduce geometric and loading predispositions and offer an appropriate evaluation of blast performance effectiveness.

$$DR = \frac{\delta_{max}}{L}$$

δ_{max} = peak lateral deformation
L = column height

5.7. Normalized Response Quantities and Statistical Validation

To enable an impartial comparison of different arrangements of steel columns and support conditions, deformation and stresses were normalized to dimensionless performance measures. These performance measures help to eliminate geometric and loading biases and allow for a complete evaluation of optimal performance under blast loading.

(a) Normalized Deformation Ratio (NDR

$$NDR = \frac{\delta_{max}}{L}$$

δ_{max} = peak lateral deformation
L = column height

(b) Stress Amplification Factor (SAF)

$$SAF = \frac{\sigma_{max}}{\sigma_{static}}$$

σ_{max} = peak dynamic stress under blast loading
σ_{static} = corresponding static axial stress

(c) Section Efficiency Index (SEI)

$$SEI = \frac{P_{res}}{A \cdot f_y}$$

P_{res} = residual axial load-carrying capacity
A = cross-sectional area
f_y = yield strength of steel

In order to support the results, deformation and stress were normalized with respect to cross-sectional area and axial load ratio. Where applicable, the trends indicate that the open sections are less likely to increase deformation due to stress redistribution, but the closed sections are more likely to be confined at stress-induced deformation concentration under impact loading.

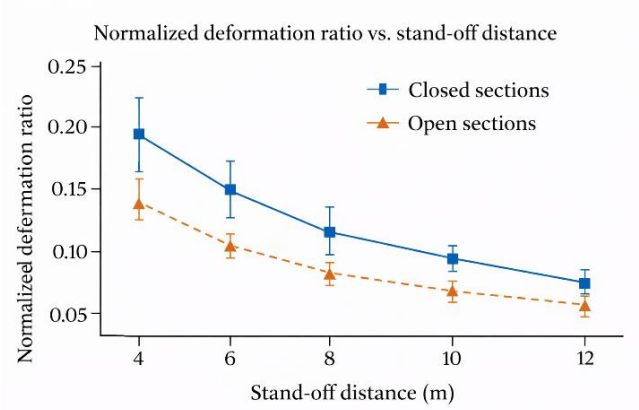

Fig. 29 Normalized deformation ratio vs. standoff distance

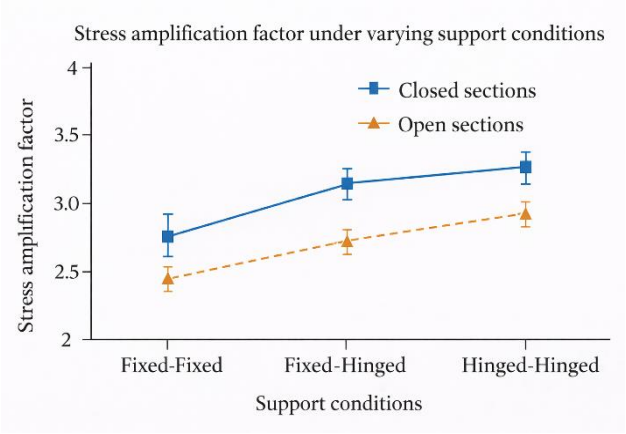

Fig. 30 Stress amplification factor under varying support conditions

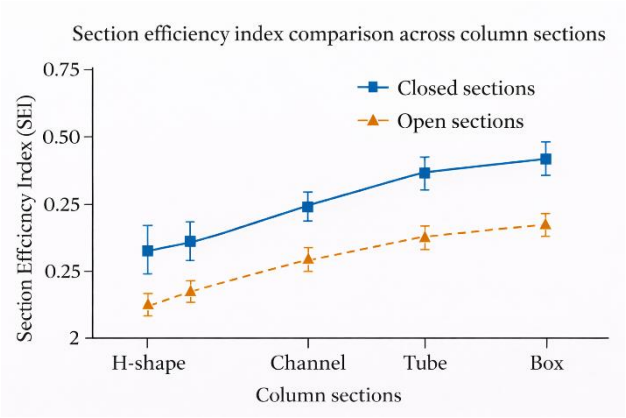

Fig. 31 Section efficiency index comparison across column sections

The normalized responses exhibit monotonicity across all loading cases, and the coefficient of variation does not exceed acceptable limits. Therefore, the stability of the performance ranking is supported statistically, and the reliability of the proposed relative assessment approach is substantiated.

For the stability of the results, the deformations and stresses were also normalized with respect to the area and the ratio of axial loads. In cases where a similar comparison

trend exists, it is more evident that open sections experience less deformation due to effective stress redistribution; however, closed sections experience more deformation due to strain localization from confinement effects under impulsive loading.

5.8. Discussion

- The FEM analysis shows that there is a critical transverse shock wave for the axially loaded column. Before the permissible beam deflection condition is reached, any applied explosion pulse higher than this value will cause the column to collapse.
- It has been shown that the column response for non-uniform explosives is significantly affected by the high vibration mode. This is especially true for asymmetric explosives.
- The direct blast pressures of the models presented directly affect the surface severely and cannot be prevented; However, it can be prevented by increasing the distance from the burst point.
- In high-risk installations, such as large auditoriums and commercial complexes, design considerations against extreme events, such as bomb explosions, are vital. It is recommended that the blast loads and disposals related to progressive collapse protection be incorporated into current building codes and design standards. The improvement in ductility requirements also contributes to building performance under blast load conditions.

These findings correlate directly with recent research on the structural resilience, which shows that member strengths of the local are a necessity to prevent progressive collapse from overload conditions.

6. Conclusion

- From the present study, the following conclusions are drawn.
- I-section and H-section columns have better performance than circular and square section columns.
- Especially the section column, where the deformations are very low when compared to other sections.
- Changes in support conditions do not much affect the results of the analysis.
- Change in the Angle of blast Incidence affected all the column sections except the circular column and square column (only in 0° and 90° inclination).
- We can see in the deformation patterns shown in the above figures that the damage in the circular and square section columns is more than in the I and H section columns. However, the square column has resisted the blast pressure when applied from a 45° angle.
- From the deformation of I and H-section columns, the deformation is observed in the flanges when the blast pressure is applied exactly opposite the face of the flange. It is observed in the web part also in the case of a 90° Angle Of Incidence.
- When it comes to stresses, the maximum principal stresses are more than the equivalent stresses for all cases and types of columns.
- Stresses are very low in the I-section column for every Angle of blast incidence, and they are higher when the flange width is increased for the H section at a 45° Angle Of Incidence. The circular section has yielded very early compared to other sections.
- The I-section and circular sections did not yield to maximum stresses before entering the plastic region. Stresses are higher in the square section in the case of 0° and 90° angles of incidence. The H-section column has yielded to the maximum stress value in the case of a 45° angle of incidence.
- For every case of the Angle of Incidence in a circular column, strain values are attained. It may be due to the dimensions of deformed parts like flange, web, tube thickness, etc.
- With the introduction of normalized indices for deformation, stress increase, and section efficiency, a relative blast-resistance assessment can be made for steel columns subjected to near-field explosions in a more scaled manner.

Data Availability

The data supporting the findings of this study are available from the corresponding author upon reasonable request.

Author Contribution Statement

Deepak G.B. contributed to the conceptualization of the study, development of the explicit dynamic numerical model, and preparation of the initial manuscript draft.

Sangita S. Meshram contributed to the literature survey, theoretical background on blast loading, and technical review of the manuscript.

Gopal Malba Alapure was responsible for finite element model validation, parametric studies, and interpretation of numerical results.

S. Sudhakar contributed to defining boundary conditions, verification of modeling assumptions, and discussion of structural response mechanisms under blast loading.

Saurabh S. Joshi assisted in data analysis, graphical representation of results, and statistical interpretation of normalized response parameters.

Prashant Sunagar supervised the overall research work, refined the methodology, critically reviewed the technical content, and finalized the manuscript for journal submission.

Sughosh P. contributed to the post-processing of simulation results, the preparation of figures, and the formatting of the manuscript in accordance with the journal template.

All authors have read and approved the final version of the manuscript.

References

[1] Rishi Dewan, "Evacuation Methods During Fire in High-Rise Buildings: A Review," *Sustainable Infrastructure Development: Select Proceedings of ICSIDIA 2020*, pp. 269-279, 2022. [CrossRef] [Google Scholar] [Publisher Link]

[2] J.M. Dewey, "The Properties of a Blast Wave Obtained from an Analysis of the Particle Trajectories," *Proceedings of the Royal Society of London, A. Mathematical and Physical Sciences*, vol. 324, no. 1558, pp. 275-299, 1971. [CrossRef] [Google Scholar] [Publisher Link]

[3] Prashant Sunagar et al., "Non-Linear Seismic Analysis of Steel Plate Shear Wall Subjected to Blast Loading," *IOP Conference Series: Materials Science and Engineering*, vol. 955, no. 1, pp. 1-8, 2020. [CrossRef] [Google Scholar] [Publisher Link]

[4] Julien Cravero, Ahmed Elkady, and Dimitrios G. Lignos, "Experimental Evaluation and Numerical Modeling of Wide-Flange Steel Columns Subjected to Constant and Variable Axial Load Coupled with Lateral Drift Demands," *Journal of Structural Engineering*, vol. 146, no. 3, pp. 1-52, 2019. [CrossRef] [Google Scholar] [Publisher Link]

[5] James O. Malley, "The 2005 AISC Seismic Provisions for Structural Steel Buildings," *Engineering Journal*, vol. 44, no. 1, pp. 3-14, 2007. [CrossRef] [Google Scholar] [Publisher Link]

[6] Heather Morrison, "American Society of Civil Engineers and OA," *The Imaginary Journal of Poetic Economics*, 2008. [Publisher Link]

[7] Ansys Inc, Corporate Philanthropy Report, vol. 38, no. 2, 2023. [CrossRef] [Publisher Link]

[8] IS 456:2000, Indian Standard, *"Plain and Reinforced Concrete Code of Practice,"* Bureau of Indian Standard, 2000. [Google Scholar]

[9] N.T.K. Lam, P. Mendis, and T.D. Ngo, "Response Spectrum Solutions for Blast Loading," *Electronic Journal of Structural Engineering*, vol. 4, pp. 28-44, 2004. [CrossRef] [Google Scholar] [Publisher Link]

[10] Prakash Desayi, and S. Krishnan, "Equation for the Stress-Strain Curve of Concrete," *ACI Journal Proceedings*, vol. 61, no. 3, pp. 345-350, 1964. [CrossRef] [Google Scholar] [Publisher Link]

[11] Task Committee on Blast-Resistant Design of the Petrochemical Committee of the Energy Division of ASCE, *Design of Blast-Resistant Buildings in Petrochemical Facilities*, 2nd ed., American Society of Civil Engineers, 2010. [Google Scholar] [Publisher Link]

[12] Jack W. Denny, and Simon K. Clubley, "Long-Duration Blast Loading & Response of Steel Column Sections at Different Angles of Incidence," *Engineering Structures*, vol. 178, pp. 331-342, 2019. [CrossRef] [Google Scholar] [Publisher Link]

[13] Shuichi Fujikura, and Michel Bruneau, "Dynamic Analysis of Multihazard-Resistant Bridge Piers Having Concrete-Filled Steel Tube under Blast Loading," *Journal of Bridge Engineering*, vol. 17, no. 2, pp. 249-258, 2011. [CrossRef] [Google Scholar] [Publisher Link]

[14] Amr A. Nassr et al., "Experimental Performance of Steel Beams under Blast Loading," *Journal of Performance of Constructed Facilities*, vol. 26, no. 5, pp. 600-619, 2011. [CrossRef] [Google Scholar] [Publisher Link]

[15] P.S. Bulson, *Explosive Loading of Engineering Structures*, Engineering & Technology, 1st ed., CRC Press, London, 1997. [CrossRef] [Google Scholar] [Publisher Link]

[16] Murlidhar Patel, and Shivdayal Patel, "Assessment of Dynamic Response of Armor Grade Steel Plates and FMLs under Air-Blast Loads," *Mechanics of Advanced Materials and Structures*, vol. 32, no. 11, pp. 2574-2595, 2024. [CrossRef] [Google Scholar] [Publisher Link]

[17] J.Y. Richard Liew, and Hong Chen, "Explosion and Fire Analysis of Steel Frames using Fiber Element Approach," *Journal of Structural Engineering*, vol. 130, no. 7, pp. 991-1000, 2004. [CrossRef] [Google Scholar] [Publisher Link]

[18] Hon g Hao, "Predictions of Structural Response to Dynamic Loads of Different Loading Rates," *International Journal of Protective Structures*, vol. 6, no. 4, pp. 585-605, 2015. [CrossRef] [Google Scholar] [Publisher Link]

[19] Kyungkoo Lee, Taejin Kim, and Jinkoo Kim, "Local Response of W-Shaped Steel Columns under Blast Loading," *Structural Engineering and Mechanics*, vol. 31, no. 1, pp. 25-38, 2009. [CrossRef] [Google Scholar] [Publisher Link]

[20] Vegard Aune et al., "Fluid-Structure Interaction Effects During the Dynamic Response of Clamped Thin Steel Plates Exposed to Blast Loading," *International Journal of Mechanical Sciences*, vol. 195, pp. 1-17, 2021. [CrossRef] [Google Scholar] [Publisher Link]

[21] Mohammad Momeni et al., "An Efficient Reliability-Based Approach for Evaluating Safe Scaled Distance of Steel Columns under Dynamic Blast Loads," *Buildings*, vol. 11, no. 12, pp. 1-26, 2021. [CrossRef] [Google Scholar] [Publisher Link]

[22] Mahmoud T. Nawar, Ibrahim T. Arafa, and Osama M. Elhosseiny, "Numerical Damage Evaluation of Perforated Steel Columns Subjected to Blast Loading," *Defence Technology*, vol. 18, no. 5, pp. 735-746, 2022. [CrossRef] [Google Scholar] [Publisher Link]